



HAL
open science

A separable prediction error method for robot identification

Mathieu Brunot, Alexandre Janot, Francisco Carrillo, Maxime Gautier

► **To cite this version:**

Mathieu Brunot, Alexandre Janot, Francisco Carrillo, Maxime Gautier. A separable prediction error method for robot identification. 7th IFAC Symposium on Mechatronic Systems (MECHATRONICS 2016), Sep 2016, Loughborough, United Kingdom. pp.487-492, 10.1016/j.ifacol.2016.10.650 . hal-01490600

HAL Id: hal-01490600

<https://hal.science/hal-01490600v1>

Submitted on 22 Mar 2017

HAL is a multi-disciplinary open access archive for the deposit and dissemination of scientific research documents, whether they are published or not. The documents may come from teaching and research institutions in France or abroad, or from public or private research centers.

L'archive ouverte pluridisciplinaire **HAL**, est destinée au dépôt et à la diffusion de documents scientifiques de niveau recherche, publiés ou non, émanant des établissements d'enseignement et de recherche français ou étrangers, des laboratoires publics ou privés.



Open Archive Toulouse Archive Ouverte (OATAO)

OATAO is an open access repository that collects the work of Toulouse researchers and makes it freely available over the web where possible.

This is an author-deposited version published in: <http://oatao.univ-toulouse.fr/>
Eprints ID: 17450

To cite this version:

Brunot, Mathieu and Janot, Alexandre and Carrillo, Francisco and Gautier, Maxime *A separable prediction error method for robot identification*. (2016) In: 7th IFAC Symposium on Mechatronic Systems, 5 September 2016 - 8 September 2016 (Loughborough University, United Kingdom).

Any correspondence concerning this service should be sent to the repository administrator: staff-oatao@listes-diff.inp-toulouse.fr

A Separable Prediction Error Method for Robot Identification

Mathieu Brunot*. Alexandre Janot**. Francisco Carrillo***. Maxime Gautier****

* ONERA, Centre Midi-Pyrénées, 2 avenue Edouard Belin, BP 74025, 31055 Toulouse Cedex 4, France (Tel: +33 562252918; e-mail: Mathieu.Brunot@onera.fr)

** ONERA, Centre Midi-Pyrénées, 2 avenue Edouard Belin, BP 74025, 31055 Toulouse Cedex 4, France (e-mail: Alexandre.Janot@onera.fr)

*** Laboratoire Génie de Production, Ecole Nationale d'Ingénieurs de Tarbes, 47 avenue d'Azereix, BP 1629, 65016 Tarbes cedex, France (e-mail: Francisco.Carrillo@enit.fr)

**** Université de Nantes, IRCCyN, 1, rue de la Noë, BP 92101, 44321 NANTES Cedex 3, France (e-mail: Maxime.Gautier@irccyn.ec-nantes.fr)

Abstract: The Prediction Error Method, developed in the field of system identification, handles the identification of discrete time noise model for systems linear with respect to the states and the parameters. However, robots are represented by continuous time models, which are not linear with respect to the states. In this article, we consider the issue of robot identification, taking into account the physical parameters as well as the noise model in order to improve the accuracy of the estimates. Thus, we developed a new technique to tackle this problem. The experimental results tend to show a real improvement in the estimation accuracy.

Keywords: Robots identification; System identification; Closed-loop identification; Predictions error methods; Output error identification.

1. INTRODUCTION

The usual method for robot identification is based on the Least-Squares (LS) technique and the Inverse Dynamic Identification Model (IDIM). The IDIM indeed allows expressing the input torque as a linear function of the physical parameters thanks to the modified Denavit and Hartenberg (DHM) notation. Therefore, the IDIM-LS method is a really practical solution, which explains its success, see (Gautier, Janot & Vandanjon 2013) and the references given therein. However this method needs a well-tuned band pass filtering to get the derivatives of the joint positions. Recently, (Janot, Vandanjon & Gautier 2014) have introduced the Instrumental Variable (IV) method which does not require such careful filtering, see an application in (Brunot et al. 2015). This method is called as IDIM-IV method. The IDIM-LS and IDIM-IV methods belong to the linear regression framework.

Another technique is the Prediction Error Method (PEM). It was originally developed in the automatic control field in the discrete time framework; see e.g. (Ljung 1999). Although this method is of great interest, it cannot be straightforwardly applied to robots, because their dynamic models are continuous time. In other words, it is about fitting Ordinary Differential Equations (ODE) coefficients, see e.g. (Schittkowski 2013) or (Baysse, Carrillo & Habbadi 2012). In robot identification, the Direct and Inverse Dynamic Identification Model (DIDIM) technique has been recently developed in (Gautier, Janot & Vandanjon 2013). It is an Output Error Method (OEM) i.e. a PEM where the noise

model filter is equal to one (the noise is assumed to be white and serially uncorrelated). Moreover, DIDIM uses the fact that the torque is linear with respect the parameters. Unlike the standard PEM method, the output of the continuous time model is simulated and not predicted; see for instance exercise 61 of (Schoukens, Pintelon & Rolain 2012).

The aim of this article is to consider the possibility of estimating the parameters of the noise filter which colours the noise, as well as the physical parameters of a robot. It has been already shown that considering PEM instead of OEM allows a better precision in the estimates (smaller covariance), see Chapter 7 of (Söderström & Stoica 1988). If the robot model is a nonlinear continuous time system, the noise filter is considered here as a linear discrete filter. In fact, it is more convenient for the identification process as explained in (Garnier, Wang & Young 2008). Two solutions to estimate this filter appear. Firstly, as with the regular PEM, the physical parameters and the filter's coefficients can be simultaneously estimated thanks to a nonlinear optimisation algorithm. Secondly, as with the Refined Instrumental Variable (see (Young 2015)), the physical parameters are estimated thanks to usual techniques, and then the filter is separately identified from the residuals. Both solutions are investigated in this article. They are evaluated through experiments. The experimental results tend to show that the separable approach seems more suitable to provide optimal estimates of the robot parameters, although the computational burden is slightly higher.

The rest of the paper is organized as follows. Section 2 reviews the usual robots identification technique IDIM-LS. Section 3 presents the PEM as developed in the field of

system identification, the OEM used for robot identification, and the proposed alternative: a separable PEM. The experimental identification of the SCARA robot is presented in Section 4. Finally, section 5 concludes this paper.

2. IDIM: INVERSE DYNAMIC IDENTIFICATION MODEL TECHNIQUE

2.1. Notations

The main notations used in this article are illustrated in Fig. 1 where z^{-1} is the unit delay operator, i.e. $z^{-1}q(t_k) = q(t_{k-1})$. The noise filter, \mathbf{H} , will always be considered as a Linear Time Invariant (LTI) system in the discrete time framework. The controller, \mathbf{C} , and the plant, \mathbf{G} , can be either continuous time or discrete time transfer functions. The input noises are considered as white and are contained in \mathbf{e} . The vector \mathbf{v} contains the measurement coloured noises.

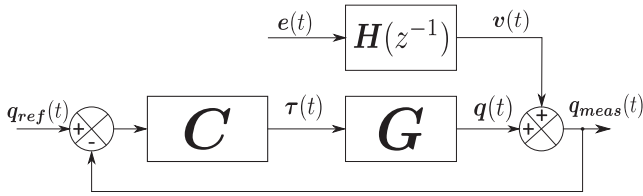


Fig. 1. Overall figure of the considered system

2.2. SCARA Prototype Model

For ease of understanding, the model of the SCARA is directly presented. To get a comprehensive picture of the robots modelling, please refer to (Khalil & Dombre 2004). SCARA (see Fig. 2) is a prototype which has previously been identified with DIDIM and IDIM-LS techniques in (Gautier, Janot & Vandanjon 2013).

The IDIM is defined by (3), where q_j , \dot{q}_j and \ddot{q}_j are respectively the angular position, velocity and acceleration of joint j . The IDIM is used for the LS identification. In the opposite, the simulation necessary for the PEM methods requires the Direct Dynamic Model (DDM), represented by the operator \mathbf{G} in Fig. 1 and given by (2). For further information about the inertia matrix \mathbf{A} , and vector \mathbf{d} (containing Coriolis and friction components), please refer to (Gautier, Janot & Vandanjon 2013) and the references given therein. The vector $\boldsymbol{\theta}$ in (1) contains the physical parameters to be estimated, where ZZ_{1r} and ZZ_2 are respectively the inertia of the first and the second link; MX_2 and MY_2 are components of the first moments of link 2; Fv_j and Fc_j are the viscous and Coulomb friction parameters of joint j .

$$\boldsymbol{\theta}^T = [ZZ_{1r} \quad Fv_1 \quad Fc_1 \quad ZZ_2 \quad MX_2 \quad MY_2 \quad Fv_2 \quad Fc_2] \quad (1)$$

$$\ddot{\mathbf{q}}(\mathbf{q}) = \mathbf{A}^{-1}(\mathbf{q}(t))(\boldsymbol{\tau}(t) - \mathbf{d}(\mathbf{q}(t), \dot{\mathbf{q}}(t))) \quad (2)$$

$$\begin{aligned} \boldsymbol{\tau}(t) &= \begin{bmatrix} \tau_1(t) \\ \tau_2(t) \end{bmatrix} = \boldsymbol{\Phi}^T(t)\boldsymbol{\theta} \\ &= [\mathbf{D}_{ZZ_{1r}} \quad \mathbf{D}_{Fv_1} \quad \mathbf{D}_{Fc_1} \quad \mathbf{D}_{ZZ_2} \quad \mathbf{D}_{MX_2} \quad \mathbf{D}_{MY_2} \quad \mathbf{D}_{Fv_2} \quad \mathbf{D}_{Fc_2}] \boldsymbol{\theta} \end{aligned} \quad (3)$$

$$\begin{aligned} \text{with, } \mathbf{D}_{ZZ_{1r}} &= \begin{bmatrix} \ddot{q}_1(t) \\ 0 \end{bmatrix}, \quad \mathbf{D}_{Fv_1} = \begin{bmatrix} \dot{q}_1(t) \\ 0 \end{bmatrix}, \quad \mathbf{D}_{ZZ_2} = \begin{bmatrix} \ddot{q}_1(t) \cos q_2(t) & \ddot{q}_2(t) \\ \dot{q}_1(t) \sin q_2(t) & \dot{q}_2(t) \end{bmatrix}, \\ \mathbf{D}_{Fc_1} &= \begin{bmatrix} \text{sign}(\dot{q}_1(t)) \\ 0 \end{bmatrix}, \quad \mathbf{D}_{Fv_2} = \begin{bmatrix} 0 \\ \dot{q}_2(t) \end{bmatrix}, \quad \mathbf{D}_{Fc_2} = \begin{bmatrix} 0 \\ \text{sign}(\dot{q}_2(t)) \end{bmatrix}, \\ \mathbf{D}_{MX_2} &= \begin{bmatrix} (2\ddot{q}_1(t) + \ddot{q}_2(t) \cos q_2(t) - \dot{q}_2(t) \sin q_2(t)) \dot{q}_1(t) + \dot{q}_2(t) \sin q_2(t) \\ \dot{q}_1(t) \cos q_2(t) + \dot{q}_2(t) \sin q_2(t) \end{bmatrix} \end{aligned}$$

and

$$\mathbf{D}_{MY_2} = \begin{bmatrix} -(2\ddot{q}_1(t) + \ddot{q}_2(t) \sin q_2(t) - \dot{q}_2(t) \cos q_2(t)) \dot{q}_1(t) + \dot{q}_2(t) \cos q_2(t) \\ \dot{q}_1(t) \cos q_2(t) - \dot{q}_2(t) \sin q_2(t) \end{bmatrix}$$

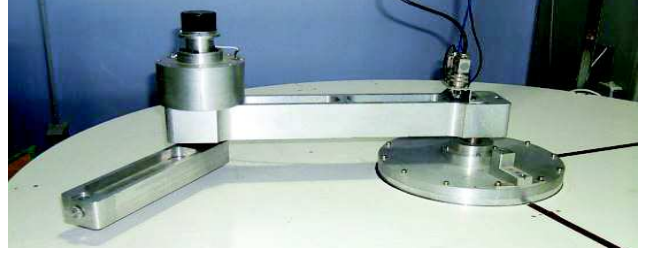


Fig. 2. SCARA Prototype

2.3. Least-Squares

The model described by (3) can be straightforwardly extended to the following vector-matrix form

$$\mathbf{u} = \boldsymbol{\Phi}\boldsymbol{\theta} + \mathbf{e}_{LS} \quad (4)$$

where, \mathbf{u} is the $(2N \times 1)$ sampled vector of $\boldsymbol{\tau}(t)$, $\boldsymbol{\Phi}$ is the $(2N \times n_p)$ sampled observation matrix of $\boldsymbol{\Phi}^T(t)$ and \mathbf{e}_{LS} is the $(2N \times 1)$ vector of error terms, with N the number of sampled data considered and n_p the number of parameters. It is assumed that $\boldsymbol{\Phi}$ is full rank, i.e. $\text{rank}(\boldsymbol{\Phi}) = n_p$, and that $N \gg n_p$, to have an over-determined system of equations.

From (4), the LS estimates and their associated covariance matrix are given by

$$\hat{\boldsymbol{\theta}}_{LS} = (\boldsymbol{\Phi}^T \boldsymbol{\Phi})^{-1} \boldsymbol{\Phi}^T \mathbf{u}, \quad \boldsymbol{\Sigma}_{LS} = \sigma_{LS} (\boldsymbol{\Phi}^T \boldsymbol{\Phi})^{-1} \quad (5)$$

$$\text{with, } \sigma_{LS} = \frac{1}{N - n_p} \sum_{k=1}^N \left\| \boldsymbol{\tau}(t_k) - \boldsymbol{\Phi}(t_k) \hat{\boldsymbol{\theta}}_{LS} \right\|^2.$$

From a theoretical point of view, the LS estimates (5) are unbiased if the error has a zero mean and if the regressors are uncorrelated with the error, see (6).

$$E(\mathbf{e}_{LS}) = 0 \quad E(\boldsymbol{\Phi}^T \mathbf{e}_{LS}) = E(\boldsymbol{\Phi}^T) E(\mathbf{e}_{LS}) = 0 \quad (6)$$

The covariance matrix given by (5) assumes that $\boldsymbol{\Phi}$ is deterministic and \mathbf{e}_{LS} is homoscedastic i.e. $\text{var}(\mathbf{e}_{LS}) = \sigma_{LS}$. It is usually assumed that those two assumptions hold.

However, the systems considered in this article operate in closed-loop. In that case, the assumption given by (6) does not hold (Van den Hof 1998). This explains why practitioners usually use tailor-made pre-filtering prior to the identification process. Various filtering approaches exist in the literature, as

for instance state variable filters, Poisson filters or implicit sensitivity filters. However, they only work for systems linear in the states, see for example (Young, Garnier & Gilson 2006). For robot identification, the usual filtering process is described in (Gautier 1997).

3. PEM: PREDICTION ERROR METHODS

3.1. Regular PEM

The original PEM has been developed to identify open-loop system, in a LTI and discrete time framework. The aim is to find the vector of parameters which minimizes the error between the measured output of the system and the predicted one. Mathematically, we must solve (7), where $\boldsymbol{\varepsilon}$ is the prediction error vector. This vector depends on the utilised technique. Different errors will be presented in this article. The problem is usually nonlinear and requires appropriate optimisation algorithm, like Levenberg-Marquardt one.

$$\boldsymbol{\theta} = \arg \min \frac{1}{2N} \sum_{k=1}^N \|\boldsymbol{\varepsilon}(t_k)\|^2 \quad (7)$$

As it has been shown in (Forssell & Ljung 1999), PEM can be extended to the closed-loop case (i.e. direct approach), but then the physical parameters and the noise model are linked. That is to say that if an error was done in the noise model identification, the estimated physical parameters would be biased, see e.g. (Forssell & Ljung 1999). This is due to the correlation between the noise, \mathbf{v} , and the input, $\boldsymbol{\tau}$. In this case, the prediction error is given by (8),

$$\begin{aligned} \boldsymbol{\varepsilon}_{pem}(t_k | \boldsymbol{\theta}) &= \mathbf{q}_{meas}(t_k) - \mathbf{q}(t_k | \boldsymbol{\theta}) \\ &= \mathbf{H}^{-1}(z^{-1}, \boldsymbol{\theta}) \left(\mathbf{q}_{meas}(t_k) - \mathbf{G}(z^{-1}, \boldsymbol{\theta}) \boldsymbol{\tau}(t_k) \right) \end{aligned} \quad (8)$$

where $\mathbf{q}(t_k | \boldsymbol{\theta})$ is the predicted output vector. The term of ‘‘predicted’’ means that it depends on $\boldsymbol{\tau}(t_i)$, with $i \in [1; k]$, but also on $\mathbf{q}_{meas}(t_j)$, with $j \in [1; k-1]$.

3.2. OEM for Robots

The standard PEM cannot be directly applied for robot identification. The robot models are indeed continuous time and nonlinear with respect to the states. This problem is similar to the one of aircraft identification; see e.g. (Klein & Morelli 2006). Both communities have developed a similar solution. Firstly, the filter that coloured the noise is usually neglected ($\mathbf{H} = \mathbf{I}$, with \mathbf{I} the identity matrix). According to the classical systems structures, see Chapter 4 of (Ljung 1999), the robots and the aircrafts are then modelled by output error models. Hence, the applied identification techniques are called OEM. Secondly, the model output is usually simulated and not predicted. Thus, the current output is function of the initial states, the past and the current inputs, but not of the past measured outputs.

As it has been seen previously, the IDIM are linear with respect to the physical parameters. We therefore consider the input torques. From this point comes the specificity of OEM in robot identification. In fact, the simulated output of the

model is $\boldsymbol{\tau}$ instead of \mathbf{q} . Thus, the output error vector is given by

$$\boldsymbol{\varepsilon}_{oem}(t_k | \boldsymbol{\theta}) = \boldsymbol{\tau}(t_k) - \boldsymbol{\tau}(t_k, \boldsymbol{\theta}) \quad (9)$$

where $\boldsymbol{\tau}(t, \boldsymbol{\theta}) = \boldsymbol{\Phi}^T(\mathbf{q}_s(t, \boldsymbol{\theta}), \dot{\mathbf{q}}_s(t, \boldsymbol{\theta}), \ddot{\mathbf{q}}_s(t, \boldsymbol{\theta})) \boldsymbol{\theta}$. The vectors \mathbf{q}_s , $\dot{\mathbf{q}}_s$ and $\ddot{\mathbf{q}}_s$ contain respectively the angular positions, velocities and accelerations of robot joints, coming from the simulation of the whole nonlinear closed-loop system. Hence, the knowledge of the controller is required for the simulation. Since the input of the simulation, \mathbf{q}_{ref} , is perfectly known (i.e. noise free), $\hat{\boldsymbol{\tau}}$ is not correlated with the measurement noise \mathbf{v} . That insures the consistency of the estimation, assuming no modelling error. Furthermore, from (3), it comes:

$$\boldsymbol{\varepsilon}_{oem}(t_k | \boldsymbol{\theta}) = \boldsymbol{\tau}(t_k) - \boldsymbol{\Phi}^T(t_k) \boldsymbol{\theta}. \quad (10)$$

If the dependence of $\boldsymbol{\Phi}$ in $\boldsymbol{\theta}$ is neglected, the optimisation of (7) is greatly enhanced. In fact, the gradient defined by (A.3), in Appendix A, is just $\boldsymbol{\Psi}(t_k, \boldsymbol{\theta}) = \boldsymbol{\Phi}^T(t_k)$. In the field of robot identification, we call it DIDIM and it is iteratively solved with LS, see Eq. (37) in (Gautier, Janot & Vandanjon 2013). In the field of system identification, this technique is called Pseudo-Linear Regression (PLR), see Eq. (7.112) in (Ljung 1999). According to the same reference, PLR is derived from (Solo 1979).

3.3. Separable PEM for Robots

The advantage of the PEM compared with the OEM is that it provides lower covariances for the estimated parameters; see e.g. Complement C7.5 in (Söderström & Stoica 1988). To achieve this in robot identification, a noise dynamics \mathbf{H} could be added in the error term (10). Nevertheless, we have no prior information about the order of the filter and this solution may lead to a complex optimization problem. Consequently, the optimization may reach local minima or even diverge. Therefore, inspired by the Refined Instrumental Variable (RIV) developed in (Young 2015), we propose a separable approach by considering the following error:

$$\boldsymbol{\varepsilon}_{sep-pem}(t_k | \boldsymbol{\theta}) = \mathbf{H}^{-1}(z^{-1}, \boldsymbol{\theta}) \boldsymbol{\varepsilon}_{oem}(t_k | \boldsymbol{\theta}). \quad (11)$$

The proposed methodology, a separable PEM (SEP-PEM), is composed by two steps:

1. Estimate the physical parameters of the system by solving (7) with (9) or (10);
2. Obtain an estimate of the noise model with (11). In other words, the residuals of the first step are used as an estimate of the noise \mathbf{v} .

Those steps are repeated until the prediction error has converged. From the residuals of the second step, an estimate of noise variance is computed with (A.2). The separation of the identification of the physical parameters and the one of the noise model implies that both models are statistically independent.

4. EXPERIMENTS

4.1. Experimental Setup

To illustrate our separable method, the SCARA prototype presented in section 2.2 is studied. The identification is performed with experimental data. Joint position and control signals are recorded with a sample frequency of 100 Hz. For the IDIM-LS method, the filters are tuned according to (Gautier, Janot & Vandanjon 2013). The first step (OEM method) is performed by solving (7) with (9), using the Levenberg-Marquardt algorithm, which is initialised with CAD values. That is to say, the inertias are approximately known (3.0 for ZZ_{1r} and 0.5 for ZZ_2) whereas all the other components are set to zero. From a practical point of view, we simulate the model with Simulink® and the parameters, solutions of (7), are found thanks to the *lsqnonlin* function, available in the Optimisation Toolbox of Matlab®. It should be noticed that the gradient is approximated using finite differences. The second step is performed with the *aic* function of the CAPTAIN Toolbox. This function seeks the Auto-Regressive filter which provides the best Akaike Information Criterion (AIC) while ensuring the withness of the estimated input signal $\hat{\mathbf{u}}$. For more detailed information about the toolbox, please refer to (Young 2011). In Eq. (11), \mathbf{H} is a (2×2) matrix of transfer functions. Since each link has its own sensor, we assume there is no correlation between the noises of both axes. That is to say that \mathbf{H} is diagonal, with $\mathbf{H}_{jj} = \frac{1}{A_{jj}(z^{-1})}$ where A_{jj} is the AR polynomial of joint j .

The robot is driven by a Proportional-Derivative (PD) controller described by (12), where Kg_1 and Kg_2 are gains equal to previously estimated inertias of the arms; $q_{j,ref}$ is the reference trajectory for arm j . Fig. 3 illustrates the joint j controller, where d_j is the nonlinear disturbance containing the friction and Coriolis terms. This is the model utilized for the simulation of the robot. Therefore, by taking $Kg_j = ZZ_{jr}$, the dynamics of the whole closed-loop system is defined just by the gains Kp_j and Kv_j . The numerical values are summarized in

Table 1. Although, the control law presents poor performances from a tracking point, it allows identifying the robot.

$$\begin{bmatrix} \tau_1(t) \\ \tau_2(t) \end{bmatrix} = \begin{bmatrix} Kg_1 \left(Kp_1 (q_{1,ref}(t) - q_{1,meas}(t)) - Kv_1 \dot{q}_{1,meas}(t) \right) \\ Kg_2 \left(Kp_2 (q_{2,ref}(t) - q_{2,meas}(t)) - Kv_2 \dot{q}_{2,meas}(t) \right) \end{bmatrix} \quad (12)$$

Table 1. Numerical values of the PD control law

	Link 1	Link 2
Kp	6.25	156.25
Kv	2.0	25.0
Kg	3.5	0.06

To insure the differentiability of the criterion, the *sign* function is not used in the simulation model. It is known that if γ is large enough then $\text{sign}(\dot{q}_j(t)) \approx 2 \arctan(\gamma \dot{q}_j(t)) / \pi$. The parameter γ is a scale factor, which is taken equal to 100. This has indeed proven to be a parsimonious choice. Actually, a too large value would make the system stiff.

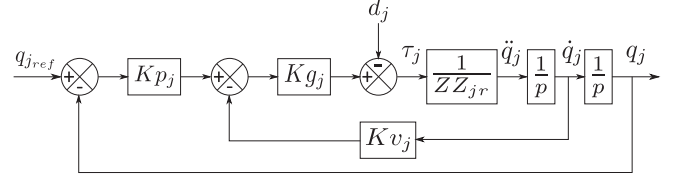


Fig. 3. PD control law of the SCARA robot, for arm j

4.2. Identification Results

The identification results are summarized in Table 2, which presents the estimated values and the relative standard deviations, defined in Appendix A. The SEP-PEM is just written PEM in the tables and figures in order to increase the readability. Since the OEM and PEM methods have estimated the same physical parameters, their results will be referred as OEM/PEM. For information, the SEP-PEM algorithm has converged in two iterations. The settings for the LS pre-filtering are the same as those in (Gautier, Janot & Vandanjon 2013). It is remarkable that LS and OEM/PEM methods provide equivalent estimates. There is a noticeable difference in the estimation of ZZ_{1r} . However, as it can be seen in Fig. 4 and Fig. 6, it does not lead to large difference in the signals estimation. In fact, with respect to Table 3, the relative errors in the torques estimations are close and satisfactory.

Table 2. Identification results

	θ_{LS}	$\% \sigma_{\theta_{LS}}$	$\theta_{OEM/PEM}$	$\% \sigma_{\theta_{OEM}}$	$\% \sigma_{\theta_{PEM}}$
ZZ_{1r}	3.50	0.007	3.44	0.024	0.0024
Fv_1	0.03	2.1	0.07	3.7	0.38
Fc_1	0.25	0.13	0.23	0.55	0.056
ZZ_2	0.06	0.040	0.06	0.13	0.013
MX_2	0.24	0.013	0.24	0.056	0.0057
MY_2	0.01	0.29	0.01	1.2	0.12
Fv_2	0.005	1.8	0.003	8.4	0.86
Fc_2	0.05	0.49	0.05	1.7	0.17

The interest of the SEP-PEM method is clearly visible in Table 2 with its small relative standard deviations. Actually, for the OEM case, the relative standard deviations are calculated with (A.2) and (9), whereas for the SEP-PEM case they are calculated with (A.2) and (11). Fig. 5 and Fig. 7 prove the efficiency of the SEP-PEM method to whiten the residuals. For information, those figures have been drawn with the *acf* function of the CAPTAIN Toolbox, with default parameters, see (Young 2011). This routine computes the AutoCorrelation Function (ACF) of the identified noise. It is recalled that for a white noise, the autocorrelation is zero for

any non-zero lag. In the presented figures, the autocorrelation values are indicated in blue (for 38 lags) and the 2σ confidence interval appears in red. The *aic* function has estimated a 13th order noise filter for the first link and 37th order one for the second link.

For the sake of completeness, we have unsuccessfully tried to identify the noise filters at the same time as the physical parameters. The filters orders and the initial values of the coefficients were those previously estimated by the *aic* function.

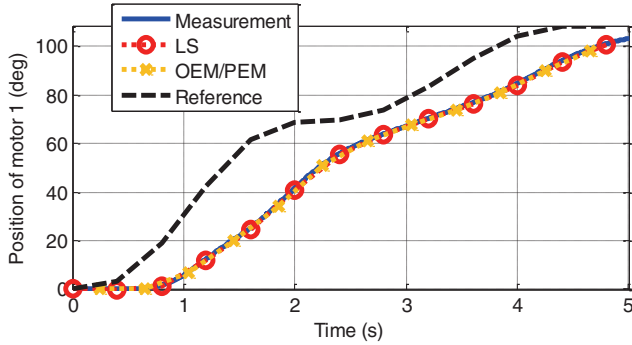
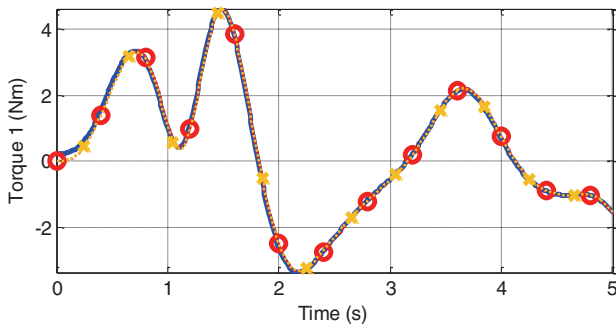


Fig. 4. Identification time history – Link 1



4.3. Cross-Validation

To validate the estimate of the SEP-PEM method, cross-validations have been performed with another experimental data set. The relative prediction errors are respectively 3.21% and 4.42% for the first and the second link. These values are equivalent to those in Table 3. Fig. 8 shows the autocorrelations of the residuals. If they seem less white than those of the identification, they are still compatible with a white noise.

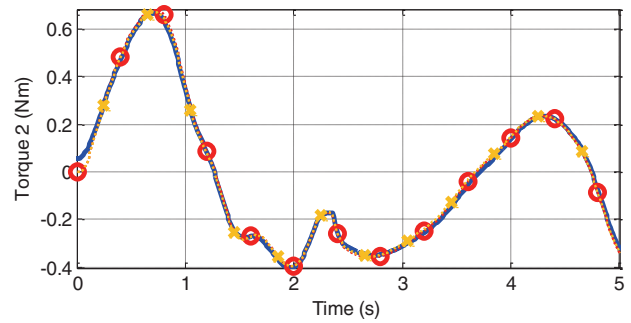
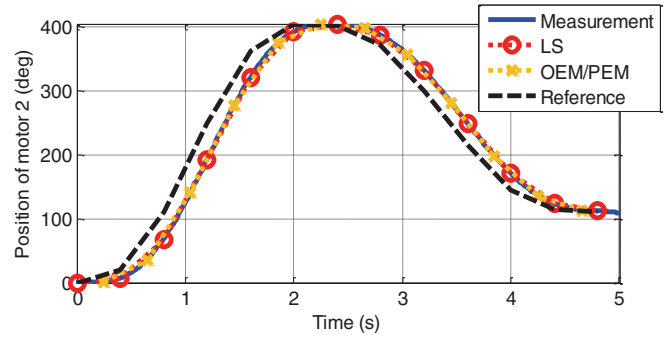


Fig. 6. Identification time history – Link 2

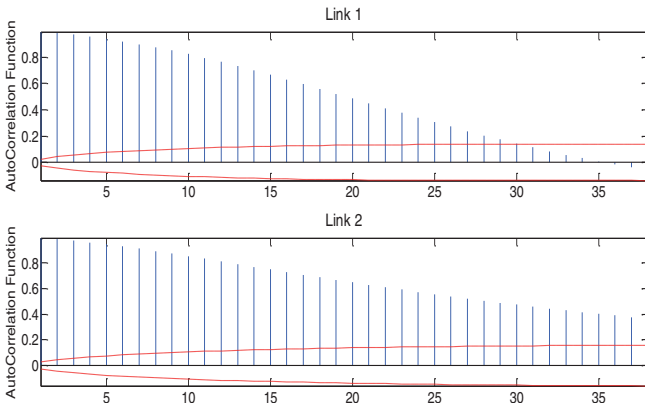


Fig. 5. Autocorrelation of the OEM residuals: Link 1 (top) and Link 2 (bottom)

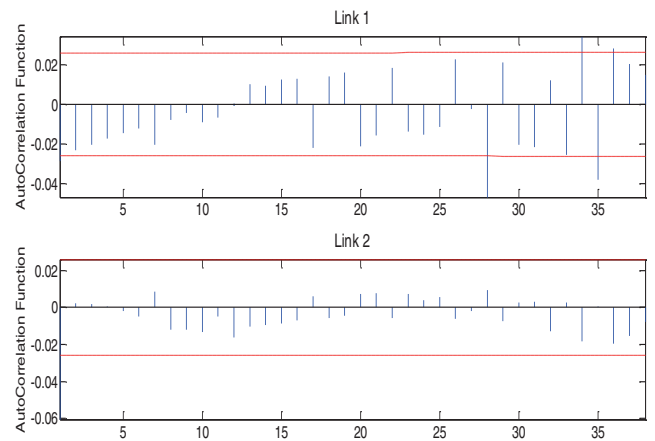


Fig. 7. Autocorrelation of the SEP-PEM residuals: Link 1 (top) and Link 2 (bottom)

Table 3. Relative estimation error

$100 \left\ \tau_{jmeas} - \hat{\tau}_j \right\ / \left\ \tau_{jmeas} \right\ $	LS	OEM/PEM
Link 1, $j = 1$	2.98%	2.39%
Link 2, $j = 2$	4.35%	4.57%

5. CONCLUSIONS

In this paper, a separable robot identification method has been presented, experimentally validated on the SCARA prototype robot and compared with two standard approaches. This technique is divided in two sequential steps: the identification of the physical parameters thanks to an output error method, and the identification of parameters of the filter, which colours the noise. The experiments carried out

with the SCARA prototype indicate that this method seems to be suitable for robot identification. Finally, compared with other standard methods, this separable approach is more effective because it provides estimates with small variances. Future works concern the application of this separable approach to an industrial robot and the comparison with other approaches not addressed in this paper.

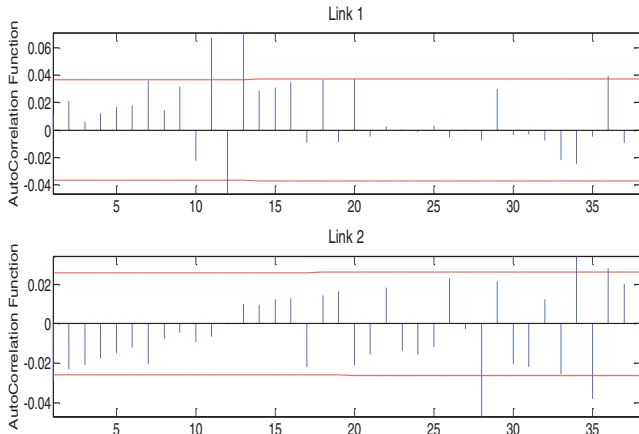


Fig. 8. Autocorrelation of the SEP-PEM residuals (cross-validation): Link 1 (top) and Link 2 (bottom)

6. REFERENCES

- Baysse, A, Carrillo, F & Habbadi, A 2012, 'Least squares and output error identification algorithms for continuous time systems with unknown time delay operating in open or closed loop', *16th IFAC Symposium on System Identification*, IFAC, Brussels.
- Brunot, M, Janot, A, Carrillo, F, Garnier, H, Vandanjon, P-O & Gautier, M 2015, 'Physical parameter identification of a one-degree-of-freedom electromechanical system operating in closed loop', *17th IFAC Symposium on System Identification*, Beijing.
- Forsell, U & Ljung, L 1999, 'Closed-loop identification revisited', *Automatica*, vol 35, no. 7, pp. 1215-1241.
- Garnier, H, Wang, L & Young, PC 2008, 'Direct identification of continuous-time models from sampled data: Issues, basic solutions and relevance', in *Identification of Continuous-time Models from Sampled Data*, Springer.
- Gautier, M 1997, 'Dynamic identification of robots with power model', *IEEE International Conference on Robotics and Automation*, IEEE, Albuquerque, NM.
- Gautier, M, Janot, A & Vandanjon, P-O 2013, 'A new closed-loop output error method for parameter identification of robot dynamics', *IEEE Transactions on Control Systems Technology*, vol 21, no. 2, pp. 428-444.
- Janot, A, Vandanjon, P-O & Gautier, M 2014, 'A generic instrumental variable approach for industrial robot identification', *IEEE Transactions on Control Systems Technology*, vol 22, no. 1, pp. 132-145.
- Khalil, W & Dombre, E 2004, *Modeling, identification and control of robots*, Butterworth-Heinemann.
- Klein, V & Morelli, EA 2006, *Aircraft system identification: theory and practice*, American Institute of Aeronautics and Astronautics, Reston, VA, USA.
- Ljung, L 1999, *System Identification - Theory for the User*, 2nd edn, Prentice Hall, Upper Saddle River, N.J.
- Schittkowski, K 2013, *Numerical data fitting in dynamical systems: a practical introduction with applications and software*, Springer Science & Business Media.
- Schoukens, J, Pintelon, R & Rolain, Y 2012, *Mastering system identification in 100 exercises*, John Wiley & Sons.
- Söderström, T & Stoica, P 1988, *System identification*, Prentice-Hall, Inc.
- Solo, V 1979, 'Time Series Recursions and Stochastic Approximation', PhD Thesis, Australian National University, Canberra, Australia.
- Van den Hof, P 1998, 'Closed-loop issues in system identification', *Annual reviews in control*, vol 22, pp. 173-186.
- Young, PC 2011, *Recursive estimation and time-series analysis: an introduction*, 2nd edn, Springer Science & Business Media, Berlin Heidelberg.
- Young, PC 2015, 'Refined instrumental variable estimation: Maximum likelihood optimization of a unified Box-Jenkins model', *Automatica*, vol 52, pp. 35-46.
- Young, P, Garnier, H & Gilson, M 2006, 'An optimal instrumental variable approach for identifying hybrid continuous-time Box-Jenkins models', *14th IFAC Symposium on System Identification, SYSID'2006*, Elsevier, Australia.

Appendix A. ASYMPTOTIC DISTRIBUTION of PARAMETERS ESTIMATES

The goal of this appendix is not to provide the whole theoretical development of Chapter 9 in (Ljung 1999), but only to remind the main results. Assuming the optimization algorithm has converged to the “true” value and there is no modelling error, the covariance matrix of the asymptotic distribution can be estimated from data by (A.1), where Ψ is the gradient defined by (A.3) and λ_N is the estimated covariance of the measurement noise.

$$\text{cov}(\theta_N) = \lambda_N \left[\sum_{k=1}^N \Psi(t_k, \theta_N) \Psi^T(t_k, \theta_N) \right]^{-1} \quad (\text{A.1})$$

$$\lambda_N = \frac{1}{N} \sum_{k=1}^N \left\| \varepsilon(t_k, \theta_N) \right\|_2^2 \quad (\text{A.2})$$

$$\Psi(t_k, \theta) = \frac{d}{d\theta} y(t_k | \theta) = -\frac{d}{d\theta} \varepsilon(t_k | \theta) \quad (\text{A.3})$$

From (A.1), it can be defined the relative standard deviation of the i^{th} parameter with (A.4), assuming non zero value.

$$\% \sigma_{\theta_i} = 100 \frac{\sqrt{\text{cov}(\theta_N)_{ii}}}{|\theta_i|} \quad (\text{A.4})$$